



CHORUS

This is the accepted manuscript made available via CHORUS. The article has been published as:

Hybridization of Higgs modes in a bond-density-wave state in cuprates

Zachary M. Raines, Valentin G. Stanev, and Victor M. Galitski

Phys. Rev. B **92**, 184511 — Published 24 November 2015

DOI: [10.1103/PhysRevB.92.184511](https://doi.org/10.1103/PhysRevB.92.184511)

Hybridization of Higgs modes in a bond-density-wave state in cuprates

Zachary M. Raines and Valentin G. Stanev
*Condensed Matter Theory Center, Department of Physics,
University of Maryland, College Park, Maryland 20742-4111, USA*

Victor M. Galitski
*Joint Quantum Institute and Condensed Matter Theory Center, Department of Physics,
University of Maryland, College Park, Maryland 20742-4111, USA and
School of Physics, Monash University, Melbourne, Victoria 3800, Australia*

Recently, several groups have reported observations of collective modes of the charge order present in underdoped cuprates. Motivated by these experiments, we study theoretically the oscillations of the order parameters, both in the case of pure charge order, and for charge order coexisting with superconductivity. Using a hot-spot approximation we find in the coexistence regime two Higgs modes arising from hybridization of the amplitude oscillations of the different order parameters. One of them has a minimum frequency that is within the single particle energy gap and which is a non-monotonic function of temperature. The other – high-frequency – mode is smoothly connected to the Higgs mode in the single-order-parameter region, but quickly becomes overdamped in the case of coexistence. We explore an unusual low-energy damping channel for the collective modes, which relies on the band reconstruction caused by the coexistence of the two orders. For completeness, we also consider the damping of the collective modes originating from the nodal quasiparticles. At the end we discuss some experimental consequences of our results.

PACS numbers: 74.72.-h,71.45.Lr

I. INTRODUCTION

Despite the decades of intense research efforts, superconductivity in cuprates remains a profound mystery. However, recently there has been a lot of progress in clarifying and refining the phase diagram of these materials experimentally.^{1,2} In particular, there is growing evidence of a charge order existing in the pseudogap state of several cuprate families,^{3–9} which also coexists and competes with superconductivity at lower temperatures. Furthermore, it appears that this order has a non-trivial d -wave phase factor,^{7,8,10} implying that within a one-band model of copper sites it describes ordering entirely on the links. For this reason it has been dubbed “bond-density wave” (BDW).¹¹ Recently, several groups employed time-domain reflectivity¹² as a tool to study this order,^{13–16} and, in particular, its collective modes. In some cases they were able to extract the amplitude and phase oscillations and to track them as the system became superconducting. These results can provide valuable insights into the physics of both pseudogap and superconducting states, and, thus, it is desirable to have a better theoretical understanding of the possible collective modes of these systems. One particularly interesting point is that the coexistence of charge order and superconductivity makes possible the direct observation of the superconducting Higgs mode, as first pointed out in the pioneering work of Littlewood and Varma.¹⁷

In this work we present a theoretical study of the Higgs modes,¹⁸ or oscillations of the amplitude,¹⁹ of the order parameters in underdoped cuprates. We consider both the pure BDW state, as well as the coexistent BDW-superconductivity phase. We use the so-called “hot-spot”

model^{20–27} of the pseudogap phase, which is based on a picture of a metallic state close to a magnetic instability, and considers the physics of the special points on the Fermi surface connected by the magnetic ordering vector. Although relatively simple, this model has seen extensive use recently, as it naturally leads to coexistence between BDW and superconductivity, and also correctly predicts the d -wave phase factor of the charge order.^{21–23}

Our results provide a general framework for identifying and understanding order-parameter collective modes of the system. In the single-order phase (i.e., only BDW or superconductivity) we find, as expected, a single amplitude mode, which is coupled with the quasiparticle continuum and is always damped. However, the coexistence regime is much more interesting – the fluctuations of the different order parameters become intertwined.¹⁷ As a consequence, in this region we find two Higgs modes, which represent coupled oscillations of the order parameters. One of the modes is slow, with frequency well below the amplitude of the order parameters, but which is, nevertheless, weakly damped. The other mode is pushed inside the high-energy continuum, and quickly becomes overdamped. We follow the slow mode in the entire coexistence phase, and find its frequency to be a non-monotonic function of temperature. This mode is weakly damped through an unusual low-energy decay channel for the antinodal quasiparticles, caused by the coexistence of the two orders and the associated band reconstruction. Even more unusually, this damping initially increases with the decrease of temperature. To account for the damping from the gapless degrees of freedom present at the nodal regions we develop a phenomenological time-dependent Ginzburg-Landau theory.

We demonstrate that, by allowing for significant damping, the in-gap mode is strongly suppressed, while the frequency of the high-energy mode is brought down. Our results provide a characterization of the amplitude modes of the coexistent superconductivity-BDW system which can be compared with the experimental data and used to identify the appropriate Higgs modes of the system.

II. MICROSCOPIC CALCULATION OF COLLECTIVE MODES FREQUENCIES

We will consider here the collective modes in a 2D “hot-spot” model. Such a model can be obtained as a low-energy theory from the 2D t-J-V model,^{20–23} which contains hoppings $t_{(1/2/3)}$ on a square lattice as well as nearest-neighbor exchange and Coulomb interactions J and V . Specifically, one projects the lattice theory onto the regions in the vicinity of 8 “hot spots” where the Fermi surface intersects the magnetic Brillouin zone boundary. In the vicinity of these hot spots the nearest-neighbor interactions J and V can be approximated by constants. Time reversal symmetry allows the problem to be reduced to considering fermions near 4 inequivalent hot spots where, in the channels of interest, the interactions take the form

$$\mathcal{H}_{\text{int}}^{\Delta} = \frac{g_s}{4} \sum_{k,p,q} \Psi_{k+q,a}^{\dagger} \check{V}_{\Delta} \Psi_{k,a} \Psi_{p-q,b}^{\dagger} \check{V}_{\Delta} \Psi_{p,b}, \quad (1)$$

$$\mathcal{H}_{\text{int}}^{\phi} = \frac{g_c}{4} \sum_{k,p,q} \Psi_{k+q,a}^{\dagger} \check{V}_{\phi} \Psi_{k,a} \Psi_{p-q,b}^{\dagger} \check{V}_{\phi} \Psi_{p,b}, \quad (2)$$

where $\Psi_{a,b}$ are Nambu spinors in pairs of hot-regions separated by the antiferromagnetic wave-vector $\vec{K} = (\pi, \pi)$ and g_s and g_c are the non-retarded components of the interaction in the superconducting and bond-density wave (BDW) channels, respectively. \check{V}_{Δ} and \check{V}_{ϕ} are the vertices for pairing in the superconducting and bond-density-wave channels. Their explicit forms for the system studied here are shown in Eq. 4.

Due to the d -wave symmetry of the order parameters one can further restrict attention to 2 of the 8 hot regions.²³ The interaction terms can be decoupled via a Hubbard-Stratonovich transformation. In the usual manner, the saddle point of the zero-frequency terms of the decoupling fields leads to a mean-field theory, which in this case has mean-field Hamiltonian

$$\mathcal{H} = \sum_{\vec{k}} \Psi_{\vec{k}}^{\dagger} \check{H}_{\text{MF}}(\vec{k}) \Psi_{\vec{k}} + \frac{2}{g_s} |\Delta|^2 + \frac{2}{g_c} |\phi|^2, \quad (3)$$

where now Ψ is a Nambu spinor $(c_{k1\uparrow}, c_{k2\downarrow}, c_{-k2\downarrow}^{\dagger}, c_{-k1\uparrow}^{\dagger})^T$ describing one pair of hot spots. The mean-field Hamiltonian describes two species (denoted 1 and 2) of spinful fermions which pair only

with each other. Specifically,

$$\begin{aligned} \check{H}_{\text{MF}} &= \check{H}_0 + \Delta \check{V}_{\Delta} + \phi \check{V}_{\phi}, \\ \check{H}_0 &= \text{diag}(\xi_1, \xi_2) \otimes \hat{\tau}_z, \\ \check{V}_{\Delta} &= \hat{\rho}_0 \otimes \hat{\tau}_1, \quad \check{V}_{\phi} = \hat{\rho}_1 \otimes \hat{\tau}_3, \end{aligned} \quad (4)$$

where $\hat{\tau}_i$ and $\hat{\rho}_i$ are Pauli matrices acting in particle-hole space and species space, respectively, and Δ describes d -wave superconductivity while ϕ is the BDW order.²³ Here, and in what follows, \check{M} denotes a matrix in the 4×4 Nambu-hot-spot space, and \hat{M} a 2×2 matrix. The self-consistency equations associated with Eq. 4 are

$$\begin{aligned} \Delta &= \frac{g_s}{4} T \sum_k \text{tr} \check{V}_{\Delta} \check{G}_k, \\ \phi &= \frac{g_c}{4} T \sum_k \text{tr} \check{V}_{\phi} \check{G}_k, \end{aligned} \quad (5)$$

where \check{G}_k is the matrix Matsubara Green’s function of the Hamiltonian in Eq. 3, which is described in Appendix A, and $k = (i\epsilon_n, \vec{k})$, with ϵ_n being a fermionic Matsubara frequency. Here we have considered Δ and ϕ to be real and non-negative (they can always be brought to this form via a gauge transformation).

In the case of a hot-spot model of cuprates, the two species correspond to fermions within a vicinity of inequivalent “hot spots” in the Brillouin zone. Close to the hot-spot points the electron dispersion can be modeled as $\xi_1(\vec{k}) = \xi_2(-\vec{k}) = v_f k_x + \gamma k_y^2$, where we include the curvature γ as it plays an important role in breaking the degeneracy between the two orders and allowing coexistence.^{23,28}

We follow Ref. 23 by choosing units where $v_f = 1$, $\gamma = 1/\Lambda = \pi$, with Λ being the hot spot cutoff, and parametrize $\{g_c, g_s\} = 3J \pm 4V$ with $J = 1.2$. Note that V strengthens the interaction in the charge channel, while decreasing the interaction in the superconducting channel,²⁹ and thus can be used to tune the coexistence (as depicted in Fig. 1). We consider two qualitatively different cases of coexisting charge order and superconductivity corresponding to the two dashed lines in Fig. 1: one where charge order disappears for some finite temperature below the superconducting T_c ($V = 0.2$), and one where charge order survives all the way down to $T = 0$ ($V = 0.21$). In both of these cases, the BDW order will onset at a temperature $T_{\text{BDW}} > T_c$. The competition between the two orders can be readily confirmed by a decrease in ϕ below the superconducting T_c .

The ordering vector of the BDW is determined by the separation in the Brillouin zone of the hot spots being paired.^{20,21,23–26} It is important to note that we are considering a BDW with ordering vector (Q, Q) , which is known to be the leading instability of this simple model.^{21,23–26} This is different from the experimentally observed bond-oriented ordering directions $(Q, 0)$ and $(0, Q)$, which correspond to a different choice of hot spots for the BDW pairing to occur between. It is possible to stabilize the $(Q, 0)$ and $(0, Q)$ orders,^{24,26,30} but at

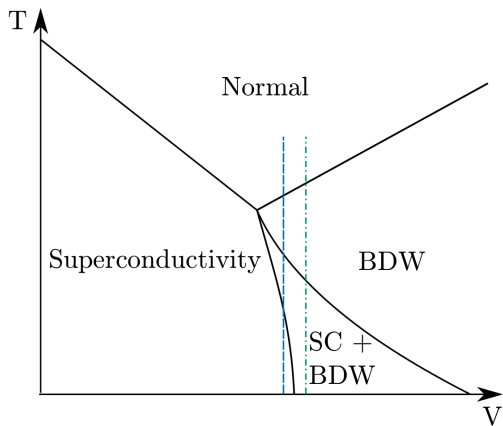


FIG. 1. (Color online) Schematic phase diagram of the hot-spot model,^{23,27} which illustrates the transition from superconductivity to charge order, tuned by V (nearest-neighbor Coulomb interaction). In this work we consider the transition from BDW to BDW-superconducting mixed state along the “trajectories” indicated by the dashed lines. Depending on the exact value of V the $T \rightarrow 0$ limit of the system could be either in a pure superconducting state (indicated by the blue dashed line), or in a mixed state (green dot-dashed line).

the price of significantly complicating the model, and we will not pursue these modifications here. We expect that most of our results and conclusions are applicable to the $(Q, 0)/(0, Q)$ orders as well.

A. Hybridized Higgs modes

The collective modes of coexisting charge-density-wave and superconducting states have been studied theoretically previously,^{17,31–36} and we apply the methods developed in these earlier works. In general, the collective modes of the system are described by a 5×5 matrix, which includes the amplitude and the phase modes of each order parameter, as well as the density oscillations of the fermions. However, this matrix factorizes into two decoupled sectors,³² with a 2×2 block describing the interacting amplitude modes, and the other 3×3 block describing the order parameters phases coupled to each other, as well as to the fermionic density.³⁷ This being the case, we devote our attention to the amplitude mode sector. In particular, we consider amplitude fluctuations of these order parameters with finite frequency ω , but zero wave-vector. Doing so allows us to calculate the mass of the collective modes: the minimum energy required to excite the collective modes of the ordered state.

Returning to the Hubbard-Stratonovich decoupling of the hot-spot model’s interactions, inclusion of the finite-frequency components of the decoupling fields leads to

the action

$$S = S_{\text{MF}} + \sum_{\vec{k}, \vec{q}, \omega_m} \bar{\Psi}_{\vec{k}+\vec{q}, \epsilon_n + \omega_m} (\Delta_{\vec{q}, \omega_m} \check{V}_\Delta + \phi_{\vec{q}, \omega_m} \check{V}_\phi) \Psi_{\vec{k}, \epsilon_n} + \frac{2}{g_s} \sum_{\vec{q}, \omega_m} |\Delta_{\vec{q}, \omega_m}|^2 + \frac{2}{g_c} \sum_{\omega_m, \vec{q}} |\phi_{\vec{q}, \omega_m}|^2, \quad (6)$$

where S_{MF} is the action corresponding to Eq. 3, which describes the mean-field state, and we are working in imaginary time. We have kept here the fluctuations $\Delta(\tau)$, $\phi(\tau)$ which are along the direction of Δ, ϕ in the complex plane,³⁸ corresponding to the amplitude modes,³⁹ which are described by the remaining terms in Eq. 6

Particularly we will be interested in the 2×2 matrix collective mode propagator

$$D_{ij}(\omega_m, \vec{q}) = \langle O_{i, \omega_m, \vec{q}} O_{j, -\omega_m, -\vec{q}} \rangle, \quad (7)$$

where $O_{1, \omega_m, \vec{q}} = \Delta_{\omega_m, \vec{q}}$ and $O_{2, \omega_m, \vec{q}} = \phi_{\omega_m, \vec{q}}$, and the related object $D_{ij}^R(\omega, \vec{q}) = D_{ij}(i\omega_m \rightarrow \omega + i0^+, \vec{q})$, which can be obtained via analytic continuation. The off-diagonal elements of this matrix are in general non-zero and this is what leads to the hybridization of collective modes. The poles of the retarded propagator \hat{D}^R will describe the on-shell collective mode energies.

After integrating out the fermionic degrees of freedom, $\hat{D}(\omega_m, \vec{q})$ can be expressed (at the quadratic level) as

$$\hat{D}^{-1}(\omega_m, \vec{q}) = (\hat{D}^0)^{-1} - \hat{Q}(\omega_m, \vec{q}), \quad (8)$$

where we have defined

$$\hat{D}^0 \equiv \frac{1}{4} \begin{bmatrix} g_s & 0 \\ 0 & g_c \end{bmatrix}. \quad (9)$$

Here Q_{ij} , also a 2×2 matrix, is the self-energy of the collective modes due to the fermionic quasiparticles (this treatment is equivalent to obtaining the generalized susceptibilities of the order parameters within the RPA approximation). Since, \hat{D}^0 is already known, \hat{Q} is the object of interest.

Specifically, \hat{Q} is given by

$$Q_{ij}(i\omega_m, \vec{q}) = -T \sum_{\vec{k}, \epsilon_n} \text{tr} \left[\check{G}(\vec{k}, \epsilon_n) \check{V}_i \check{G}(\vec{k} - \vec{q}, \epsilon_n - \omega_m) \check{V}_j \right], \quad (10)$$

where $i, j \in \{\Delta, \phi\}$. After performing the fermionic Matsubara sums in Eq. 10 we analytically continue the bosonic frequency to the real axis, in order to obtain the finite-temperature, retarded self-energy $Q^R(\omega, \vec{q})$.⁴⁰

The long-wavelength frequencies of the amplitude modes are given by the solutions of

$$\det[(\hat{D}^0)^{-1} - \hat{Q}^R(\omega_0 - i\Gamma_0, \vec{q} \rightarrow 0)] = 0, \quad (11)$$

where

$$\omega_0 \equiv \text{Re}[\omega(q \rightarrow 0)], \quad (12)$$

$$\Gamma_0 \equiv -\text{Im}[\omega(q \rightarrow 0)], \quad (13)$$

are, respectively, the mass and the decay rate of the Higgs mode in the long wavelength limit. The in-gap collective modes, are those for which $\omega_0 < 2 \min(\phi, \Delta)$.

One can explicitly show that the diagonal components of \hat{Q}^R reproduce the usual $2\phi/2\Delta$ amplitude modes¹⁷ in the limit where one of the order parameters vanishes. However, in our case, we focus our attention on the eigenmodes of the response function, which describe hybridized modes of the system⁴¹ and which cannot be obtained from purely considering the superconducting and BDW susceptibilities.

Because we are interested in weakly damped oscillations such that it makes sense to describe them as collective modes, we are able to employ a technique to determine the complex frequency of the oscillations from considerations of the response function on the real frequency line. In particular, we obtain the real part of the frequency as the solution to the equation $\text{Re}[\lambda(\omega_0)] = 0$ where λ is a solution to the eigenvalue problem

$$\left[(\hat{D}^0)^{-1} - \hat{Q}^R(\omega) - \lambda(\omega) \hat{I} \right] \begin{pmatrix} \Delta_\omega \\ \phi_\omega \end{pmatrix} = 0. \quad (14)$$

The imaginary part of the frequency can then be calculated by expanding the eigenvalue as a function of complex ω about the real frequency.^{31,42} We defer analysis of the imaginary part (shown in Fig. 3) until Sec. II B and focus now on the real part.

In order to track the temperature dependence of the collective modes, we explicitly solve the mean field equations for a range of temperatures and then calculate the collective mode frequencies at each temperature. Below T_{BDW} , in the pure BDW phase, we find an amplitude mode starting at frequency 2ϕ , as expected.¹⁷ With the onset of superconductivity, another mode appears inside the gap. Physically, it represents coupled oscillations of the two order parameters, wherein pairs are excited in both the BDW and superconducting channels. The mixing of the two orders arises due to the off-diagonal elements of \hat{Q}^R , proportional to $\phi\Delta$. Intuitively, one might anticipate the presence of such an in-gap mode by arguing that one could convert one type of pairing into the other at a smaller energy than it would take to completely break a pair.

The temperature dependence of the mode's frequency is non-trivial – initially it grows, but then reaches a maximum and goes down with the decrease of either ϕ or Δ . Depending on the shape of the coexistence region, this mode either survives all the way down to $T = 0$ or it vanishes at the second transition to a single-order-parameter phase. This behavior can be seen in Fig. 2. Note that near the phase transitions, this mode approaches the $2\phi/2\Delta$ amplitude mode of the order that vanishes at that temperature, which is the reason for the softening of the mode in the vicinity of these points.

At the onset of the coexistent phase, the other (2ϕ) mode is pushed to higher energies, enters the quasiparticle continuum, and quickly becomes overdamped. Thus,

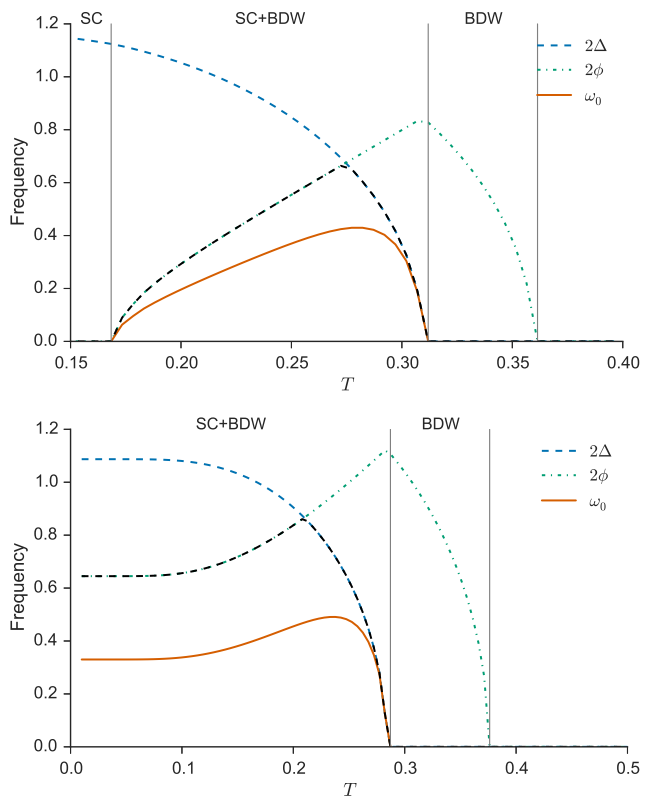


FIG. 2. (Color online) Mass of the in-gap hybrid Higgs mode $\omega_0 = \text{Re}[\omega(q \rightarrow 0)]$ as obtained from Eq. 11. The frequency is plotted as a function of temperature for two different cases of $\phi(T \rightarrow 0)$ ($V = 0.2, 0.21$) as depicted by the dashed lines in Fig. 1, using the units of Ref. 23. A soft mixed mode emerges in both cases below the superconducting T_c . For reference, twice the single-particle energy gap, which is determined by $2 \min(\Delta, \phi)$, is plotted in the black dashed line. In proximity of a phase transition, the in-gap mode approaches the $2\Delta/2\phi$ Higgs mode of the vanishing order.

it is outside the region of validity of our method of finding ω , and so we do not track it.

B. Damping from antinodal quasiparticles

As explained in Sec. II A, the damping rate Γ_0 , can be obtained by expanding the eigenvalues of Eq. 14 about the real part of the zero momentum dispersion ω_0 . The temperature dependence of this damping rate is shown in Fig. 3. Although the in-gap mode stays below the $(2\Delta, 2\phi)$ threshold, its frequency has a finite damping rate, which, furthermore, initially *increases* as temperature goes down. This unusual behavior of the damping arises from the BDW bubble $Q_{\phi\phi}^R$: when just charge order is present, the only scattering which could lead to damping requires at least energy 2ϕ (as can be seen in Fig. 4a). All other types of scattering have zero matrix element, and thus there is no damping at $q = 0$ for

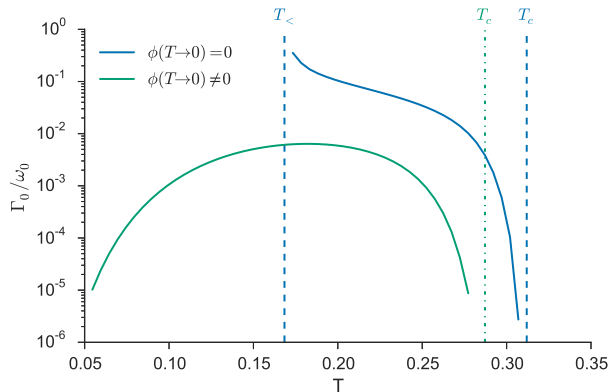


FIG. 3. (Color online) Damping rate Γ_0 of the in-gap collective mode in the long wavelength limit for two different values of V corresponding to the two trajectories depicted in Fig. 1. Damping is an order of magnitude smaller in the case where $\phi(T \rightarrow 0) \neq 0$ (lower line), and is exponentially suppressed at low temperature due a lack of thermally excited quasiparticles. In both cases, the decay rate is strongly suppressed in the vicinity of the superconducting T_c . The transition temperatures are marked for $\phi(T \rightarrow 0) = 0$ ($\phi(T \rightarrow 0) \neq 0$) by the dashed (dot-dashed) vertical lines. T_c denotes the onset temperature of superconductivity, while $T_<$ indicates the boundary between the coexistent and pure superconductivity phases (c.f. the upper plot of Fig. 2).

$\omega_0 < 2\phi$. However, as soon as Δ becomes non-zero the bands are reconstructed due to hybridization of the BDW bands with their corresponding hole bands, and simultaneously scattering matrix elements between all bands become non-zero, allowing transitions between any two bands to contribute (c.f. Fig. 4b). As a result, there now exist transitions for arbitrarily small frequency (between the two particle/hole bands), giving rise to the damping of collective modes within the gap.

The specific temperature dependence of the damping results from a combination of two effects. Because we are considering energies $\omega_0 < 2 \min(\phi, \Delta)$, we see that transitions from a particle to a hole band (or vice versa) cannot contribute as they will always have energy equal or greater than 2Δ . Thus, damping must be solely due to scattering between the hole or particle bands. As ϕ decreases, the two particle (and correspondingly the two hole) bands become more similar (in the limit $\phi \rightarrow 0$ they are degenerate), increasing the phase space for low energy transitions and therefore leading to greater damping of the BDW amplitude mode. This in turn leads to an increased damping of the mixed mode, which is visible in Fig. 3. However, in opposition to this effect, as $\phi \rightarrow 0$, the matrix element for scattering between these bands will begin to vanish, as it is proportional to ϕ . At some point this second effect will overcome the increase due to the larger phase space, leading to a disappearance of the damping as we approach the critical point at which the charge order disappears.

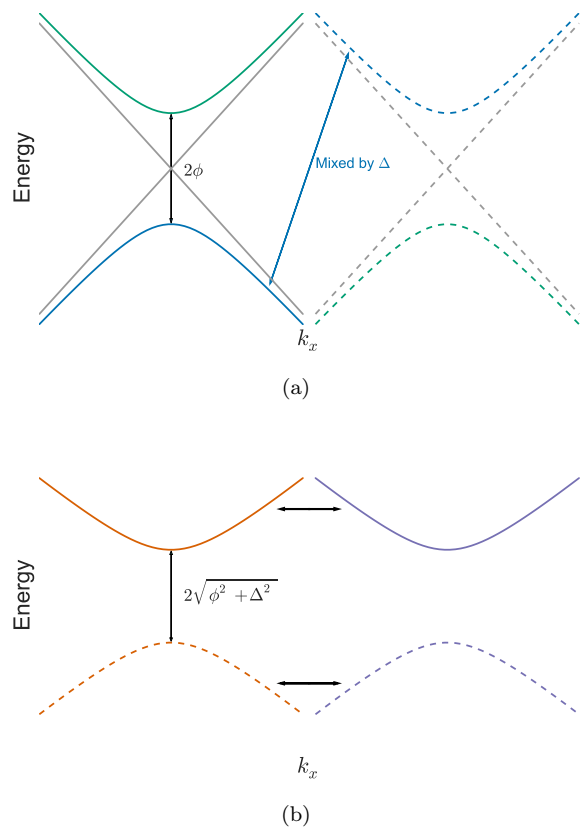


FIG. 4. (Color online) Slices of the quasiparticle band structure for $k_y = 0$. Dashed lines indicate the particle hole conjugate of the band of the same color. (a) The normal state (gray) and BDW state (green/blue) dispersions. Only transitions between the two solid/dashed bands contribute to $\text{Im}Q_{\phi\phi}^R$. The onset of superconductivity hybridizes the green/blue bands with their particle-hole conjugates. (b) Bogoliubov band dispersions in the coexistent state. Transitions between all bands may contribute to $\text{Im}Q_{\phi\phi}^R$ leading to damping of the Higgs modes (even for those with mass less than 2Δ). Processes indicated by horizontal arrows are of particular importance as they occupy a finite phase space for arbitrary frequencies within the gap.

The competition between scattering elements and band structure generically leads to a non-monotonic temperature dependence of the damping, which in turn means that there exists a region of maximal damping away from which the decay rate remains weak (within the gap). In the case with $\phi(T \rightarrow 0) \neq 0$, the BDW order remains sufficiently large that the system never approaches this region of larger damping and thus the decay rate is noticeably smaller than for $\phi(T \rightarrow 0) = 0$. In all cases where the mixed phase exists down to $T = 0$, this damping term will be exponentially suppressed at low temperatures as there are no thermally excited quasiparticles available to scatter.

III. DAMPING FROM NODAL QUASIPARTICLES

The hot-spot model we have used so far is only defined in the antinodal regions, and thus completely ignores the gapless degrees of freedom existing close to the nodes. These can have a particularly strong effect on the damping of the collective modes by providing a low-energy decay channel. However, the contribution of these quasiparticles is different for the different orders. We expect the charge order to couple only weakly to the nodal quasiparticles, due to the mismatch between its wavevector (Q, Q) and the wavevector separating the nodes⁴³ [note that the same argument applies to BDW with $(Q, 0)$ or $(0, Q)$ wavevector]. There is no such restriction for the superconductivity, however, and its amplitude fluctuations are unavoidably damped by the nodal excitations. To include these effects and to study their consequences for the collective modes, we supplement the calculation from the previous section with a phenomenological time-dependent Ginzburg-Landau theory. In addition to the more familiar quadratic and quartic in the order parameters terms, this theory contains also first and second derivatives in (real) time. The time-dependent Ginzburg-Landau equations can be written in the following form:⁴⁴

$$\begin{aligned} -\frac{\partial^2 \Delta}{\partial t^2} - \gamma_\Delta \frac{\partial \Delta}{\partial t} &= \frac{\partial \mathcal{F}_{GL}}{\partial \Delta^*}, \\ -\frac{\partial^2 \phi}{\partial t^2} - \gamma_\phi \frac{\partial \phi}{\partial t} &= \frac{\partial \mathcal{F}_{GL}}{\partial \phi^*}, \end{aligned} \quad (15)$$

where the Ginzburg-Landau action is given by:

$$\mathcal{F}_{GL} = \alpha_\phi |\phi|^2 + \alpha_\Delta |\Delta|^2 + \beta_\phi |\phi|^4 + \beta_\Delta |\Delta|^4 + u |\phi|^2 |\Delta|^2.$$

The quadratic coefficients α have the usual linear-in-temperature dependence, whereas β and u (which parametrises the competition between the two orders) are temperature-independent.⁴⁵ Note that expressions for the coefficients in \mathcal{F}_{GL} can be straightforwardly derived from the microscopic theory presented in the previous section⁴⁶ (spatial derivative terms are not included since we are considering only uniform states). Although the Ginzburg-Landau theory is strictly applicable only close to the critical region, it can be used beyond its region of validity as an effective model for the collective modes of the system.¹⁹ For this reason we keep the second-order time derivative terms, which are usually omitted close to the critical temperature.⁴⁷

The coefficients γ_ϕ and γ_Δ are responsible for the damping of the collective modes. It is important to note that despite the symmetric way these terms enter Eq. 15, they encode very different physics. The γ_ϕ term is native to the hot-spot regions. At low energies it is proportional to Δ , since it is only allowed by the band reconstruction (see the discussion in the previous section), whereas above $2 \min(\Delta, \phi)$ we can treat it as a constant, originating from the coupling of the fluctuations to the high-energy quasiparticle continuum. In contrast, the main

contribution to the γ_Δ term originates from the nodal regions (and thus is completely absent in the hot-spot-only approach of the previous section). Close to T_c we can obtain its temperature dependence from the following qualitative considerations. This term is proportional to the number of available states at the oscillation frequency, given by $\sim \rho(\omega) \tanh(\omega/4T)$.⁴⁸ Linearizing the density of states close to the nodes $\rho(\omega) \sim \omega$, and approximating the frequency as $\omega \approx 2\Delta$ we finally get for the damping terms of the slow mode

$$\gamma_\Delta \approx \gamma_\Delta^0 \Delta^2 = \gamma_\Delta^0 (T_c - T), \quad \gamma_\phi \approx \gamma_\phi^0 \Delta = \gamma_\phi^0 \sqrt{T_c - T}$$

(we have expanded in powers of Δ). Note that we have thus determined the temperature dependence of γ_ϕ and γ_Δ , but their relative strength at some fixed temperature depends on the parameters of the microscopic models (like V), which cannot be estimated within our phenomenological theory. However, given the general temperature dependence of γ_ϕ and γ_Δ , we expect the antinodal particles to dominate damping sufficiently close to T_c (Δ vs. Δ^2), whereas at low temperatures the nodal excitations take over – γ_Δ stays finite for $T \rightarrow 0$, while γ_ϕ goes to zero exponentially.

To obtain the frequencies and damping of the mixed modes we expand $\phi(t)$ and $\Delta(t)$ around the mean field values of the order parameters ϕ_0 and Δ_0 : $\phi(t) = \phi_0 + \delta\phi(t)$ and $\Delta(t) = \Delta_0 + \delta\Delta(t)$. Assuming that $\delta\phi(t)$ and $\delta\Delta(t)$ are relatively small we can simplify Eq. 15 by keeping only the terms linear in $\delta\phi$ and $\delta\Delta$. Since we are interested in the collective modes we write their time dependence as $e^{-i\omega t}$. Inserting this ansatz in the linearized equations, we can exclude $\delta\phi$ and $\delta\Delta$ altogether, and finally arrive at the following equation for ω :

$$\omega^2 + i\gamma_\phi \omega + 2(\alpha_\phi + u\Delta_0^2) - \frac{(2u\phi_0\Delta_0)^2}{2(\alpha_\Delta + u\phi_0^2) + i\gamma_\Delta \omega + \omega^2} = 0. \quad (16)$$

We solve it numerically (with $\phi_0(T)$ and $\Delta_0(T)$ determined by the time-independent mean-field equations), and obtain both complex and purely imaginary solutions for ω . The former solutions are oscillatory (with $\text{Re}[\omega]$ giving the frequency of the uniform oscillations around the mean field values), while the latter represent exponential decay. We show the real and the imaginary parts of the two ω solutions as a function of temperature in Fig. 5. There we plot ω_0 and Γ_0 for two different strengths of γ_Δ^0 , as a comparison between small and large contribution from the nodal quasiparticles, respectively. For small γ_Δ^0 we can see that both the real and imaginary parts of the frequency of the hybridized modes show behavior similar to that obtained in the previous section. However, when we increase γ_Δ^0 we see not only enhancement of the damping of both modes, but also decrease of their real frequencies (the top panel of Fig. 5). Although the effect is more dramatic for the in-gap mode, which now exists only in a narrow region below T_c , it is

significant for the fast one as well. This is a consequence of one important feature of Eq. 16 – the coupling of the two channels mixes their real and imaginary parts. Thus, increase of the damping leads to the gradual suppression of the real part of both mixed modes. Note also that the disappearance of ω_0 of the in-gap mode corresponds to a peak in its Γ_0 .

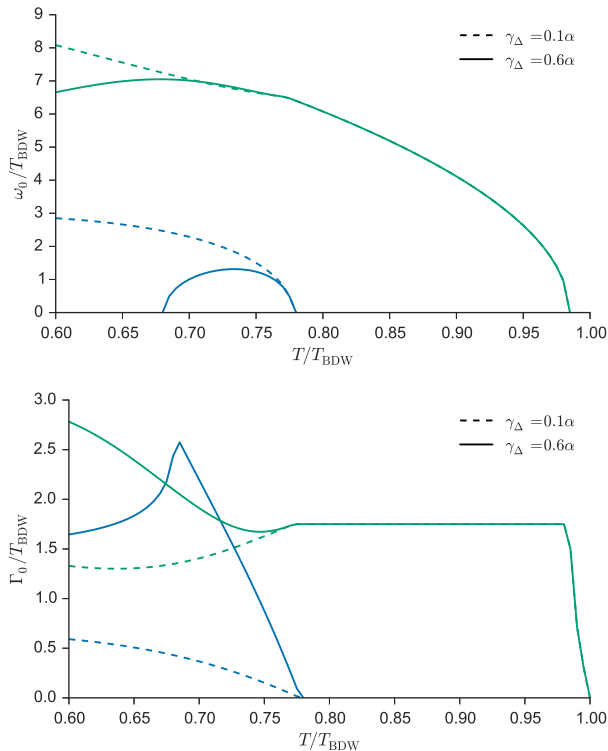


FIG. 5. (Color online) The evolution of ω_0 (top panel) and Γ_0 (bottom panel) of the two Higgs modes with temperature. For each mode the cases of weak and strong damping from the nodal regions are shown [$\gamma_\Delta = 0.1\alpha$ (dashed line) and $\gamma_\Delta = 0.6\alpha$ (solid line), respectively]. γ_ϕ , the damping from antinodal region, is the same on both plots.

IV. DISCUSSION AND CONCLUSION

Note that our calculation is to some extent complementary to those in Refs. 28 and 49. These works studied the dynamics of the system after an external perturbation, and were done in the time domain, thus allowing direct comparison with the experimental data. The temperature dependence of the frequencies extracted in Ref. 49 appears consistent with our calculation, as it shows a low-frequency mode appearing below the superconducting transition.

The experiments^{14–16} have not observed a soft mode close to either charge or superconducting transition temperatures. Instead, Refs. 14 and 15 identify a single amplitude mode, with intensity that goes down with temper-

ature, but whose frequency stays almost constant, with only a small decrease at the superconducting T_c observed in Ref. 14, and no clear change seen in Ref. 15.⁵⁰ In contrast to these, Ref. 16 reported two collective modes at the wavevector corresponding to the charge order, with one of them disappearing close to the superconducting transition (the other – higher-frequency – one follows behavior similar to that observed in Refs. 14 and 15). This seems to be a direct confirmation of the coupling between the charge order and superconductivity, and in agreement with our theory. However, the frequency of this mode remains constant with temperature, without any signs of softening. The absence of softening close to either T_c or T_{BDW} appears incompatible with our calculation, and requires alternative explanations (such as optical phonons).¹⁴

There remains an important point regarding the experimental signatures of the amplitude modes. Since the superconducting Higgs mode does not directly couple to the electromagnetic field (although it could be detected by indirect methods⁵¹), the mixing provides a convenient way of observing it. However, it can be easily shown that the soft mode’s coupling to reflectivity is proportional to Δ_0 , and is thus small just below the superconducting transition. Combined with the fact that damping from the nodal regions can restrict this mode to a small region in the vicinity of the superconducting transition (as explored in Sec. III), this might explain why some groups^{14,15} have not observed a low-frequency mode at temperatures below the superconducting T_c .

In conclusion, we have studied the collective modes for the bond density wave and superconducting order parameters expected to exist in the pseudogap state of cuprates. In the pure BDW phase we observed the conventional amplitude mode with frequency starting at 2ϕ . In the coexistent phase two collective modes representing the coupled oscillations of the order parameters are present. One of them is soft at the superconducting critical temperature, and despite having frequency $\omega_0 < 2 \min(\phi, \Delta)$ is (weakly) damped, due to band-structure reconstruction caused by superconductivity. The other mixed mode is continuously connected to the pure BDW mode, with frequency pushed up in the coexisting regime. To study the effects of damping originating from the nodal regions, we developed a phenomenological time-dependent Ginzburg-Landau theory. We demonstrated that strong damping can have significant effect on the real frequency of the modes.

ACKNOWLEDGMENTS

We are grateful to D.H. Torchinsky for enlightening discussion, and S. Sachdev and G. Volovik for helpful comments. This work was supported by U.S. Department of Energy BES-DESC0001911 and Simons Foundation.

Appendix A: Mean-field Nambu Green's function

The matrix Matsubara Green's function of Eq. 3 can be obtained by two consecutive Bogoliubov transformations in subspaces of the Nambu-spinor matrix structure. Doing so allows for the Green's function to be written in terms of the eigenvalues of the Hamiltonian as

$$\check{G}_k = \check{U}_k \check{g}_k \check{U}_k^\dagger, \quad (\text{A1})$$

$$\check{g}_k^{-1} = i\epsilon_n \check{1} - \text{diag}(E_k^+, E_k^-, -E_k^+, -E_k^-), \quad (\text{A2})$$

where the energies of the Bogoliubov quasiparticles are given by

$$\begin{aligned} E^\pm &= \sqrt{(\lambda^\pm)^2 + \Delta^2}, \\ \lambda^\pm &= \xi_\pm \pm \sqrt{\xi_-^2 + \phi^2}, \\ \xi_\pm &= \frac{\xi_1 \pm \xi_2}{2}. \end{aligned} \quad (\text{A3})$$

The diagonalization matrix can be written in terms of the matrices

$$\begin{aligned} \hat{A} &= \begin{bmatrix} w & -z \\ z & w \end{bmatrix}, \\ w &= \sqrt{\frac{1}{2} \left[1 + \xi_- (\xi_-^2 + \phi^2)^{-1/2} \right]}, \\ z &= \sqrt{\frac{1}{2} \left[1 - \xi_- (\xi_-^2 + \phi^2)^{-1/2} \right]}, \end{aligned} \quad (\text{A4})$$

and

$$\begin{aligned} B^\pm &= \begin{bmatrix} u^\pm & -v^\pm \\ v^\pm & u^\pm \end{bmatrix} \\ u^\pm &= \sqrt{\frac{1}{2} \left(1 + \frac{\lambda^\pm}{E^\pm} \right)}, \\ v^\pm &= \sqrt{\frac{1}{2} \left(1 - \frac{\lambda^\pm}{E^\pm} \right)}, \end{aligned} \quad (\text{A5})$$

as

$$\begin{aligned} \check{U} &= \left(\hat{A} \otimes \hat{\tau}_0 \right) \left(\sum_{\pm} \hat{P}^\pm \otimes \hat{B}^\pm \right), \\ \hat{P}^\pm &= \frac{1}{2} (\hat{\rho}_0 \pm \hat{\rho}_3). \end{aligned} \quad (\text{A6})$$

Appendix B: Effect of phonons

Beyond just the non-retarded interaction considered above, one can also consider the effect of phonons on the collective modes. Here we will take this into account by considering the contribution of the frequency dependent phonon-mediated interaction between electrons to the collective mode propagators. In particular, we will project this interaction onto a hot spot model by taking

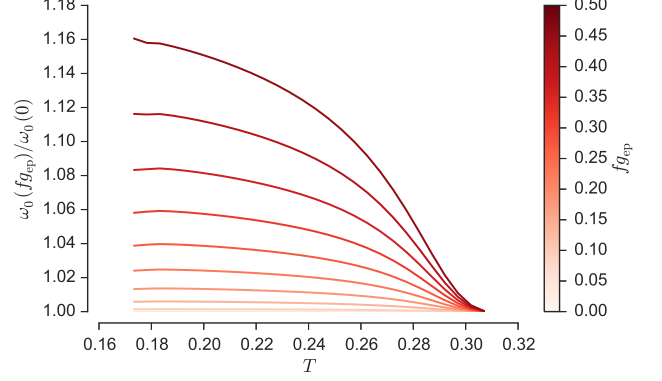


FIG. 6. (Color online) The in-gap collective mode mass ω_0 (relative to the $g_{\text{ep}} = 0$ case) as a function of the electron phonon coupling g_{ep} , for $\Omega_Q = 1$. The $g_{\text{ep}} = 0$ line corresponds to the behavior shown in Fig. 2.

the phonon momentum to be the fixed wavevector \vec{Q} separating the hot spots which are being paired – this is the same approximation that one uses on the non-retarded interaction in deriving the hot spot model.

A simple A_{1g} symmetry phonon has no effect on the collective modes due to the pure d -wave symmetry of the order parameters. However, in reality we expect some direct order parameter-phonon coupling, either because there is a phonon mode with the correct symmetry (B_{1g}), or because in real systems the order parameter would not necessarily have a pure d -wave symmetry, but could have an s -wave component admixed. Regardless of the exact nature of the coupling, it gives rise to a term in the mean field theory which includes the phonon-mediated interaction as

$$\begin{aligned} H_{ph} &= f \sum_{k, \epsilon_n, \omega_m} U(\omega_m) \\ &\times \left(\phi(\omega_m) c_{1\sigma}^\dagger(k, \epsilon_n - \omega_m) c_{2\sigma}(k, \epsilon_n) + h.c. \right) \end{aligned} \quad (\text{B1})$$

where

$$U(\omega_m) = \frac{g_{\text{ep}}^2}{2} \frac{\Omega_Q}{\omega_m^2 + \Omega_Q^2}$$

is an Einstein phonon type propagator and f is a constant of order one arising from the form factor of the electron-phonon vertex.

If we consider the effect of this term on the charge collective mode, we find that it can be captured by the replacement $g_c \rightarrow \tilde{g}_c(i\omega_m)$. We absorb the $\omega = 0$ component into the definition of g_c (as that is what determines the static mean-field solution) and include the remaining frequency dependent part in our calculation of the collective modes. Upon analytic continuation to real frequency, this amounts to the substitution

$$g_c \rightarrow \tilde{g}_c(\omega) = g_c - \frac{f g_{\text{ep}}^2}{\Omega} - f g_{\text{ep}}^2 \frac{\Omega}{\omega^2 - \Omega^2} \quad (\text{B2})$$

in the collective mode equations (the additive constant is chosen so that we recover $\tilde{g}_c(\omega = 0) = g_c$). The previous analysis can now be repeated for a range of electron phonon couplings. As can be seen in Fig. 6, the cou-

pling to phonons tends to push the collective mode mass slightly upward, while leaving the softening at the phase transitions unmodified. Overall, the qualitative behavior of the mode is not markedly different.

-
- ¹ L. Taillefer, *Annu. Rev. Condens. Matter Phys.* **1**, 51 (2010).
- ² B. Keimer, S. a. Kivelson, M. R. Norman, S. Uchida, and J. Zaanen, *Nature* **518**, 179 (2015).
- ³ G. Ghiringhelli, M. Le Tacon, M. Minola, S. Blanco-Canosa, C. Mazzoli, N. B. Brookes, G. M. De Luca, A. Frano, D. G. Hawthorn, F. He, T. Loew, M. M. Sala, D. C. Peets, M. Salluzzo, E. Schierle, R. Sutarto, G. A. Sawatzky, E. Weschke, B. Keimer, and L. Braicovich, *Science* **337**, 821 (2012).
- ⁴ J. Chang, E. Blackburn, A. T. Holmes, N. B. Christensen, J. Larsen, J. Mesot, R. Liang, D. A. Bonn, W. N. Hardy, A. Watenphul, M. V. Zimmermann, E. M. Forgan, and S. M. Hayden, *Nat. Phys.* **8**, 871 (2012).
- ⁵ A. J. Achkar, R. Sutarto, X. Mao, F. He, A. Frano, S. Blanco-Canosa, M. Le Tacon, G. Ghiringhelli, L. Braicovich, M. Minola, M. Moretti Sala, C. Mazzoli, R. Liang, D. A. Bonn, W. N. Hardy, B. Keimer, G. A. Sawatzky, and D. G. Hawthorn, *Phys. Rev. Lett.* **109**, 167001 (2012).
- ⁶ G. Coslovich, C. Giannetti, F. Cilento, S. Dal Conte, T. Abebaw, D. Bossini, G. Ferrini, H. Eisaki, M. Greven, A. Damascelli, and F. Parmigiani, *Phys. Rev. Lett.* **110**, 107003 (2013).
- ⁷ K. Fujita, M. H. Hamidian, S. D. Edkins, C. K. Kim, Y. Kohsaka, M. Azuma, M. Takano, H. Takagi, H. Eisaki, S.-i. Uchida, A. Allais, M. J. Lawler, E.-A. Kim, S. Sachdev, and J. C. S. Davis, *Proc. Natl. Acad. Sci.* **111**, E3026 (2014).
- ⁸ R. Comin, R. Sutarto, F. He, E. H. da Silva Neto, L. Chauviere, A. Frano, R. Liang, W. N. Hardy, D. A. Bonn, Y. Yoshida, H. Eisaki, A. J. Achkar, D. G. Hawthorn, B. Keimer, G. A. Sawatzky, and A. Damascelli, *Nat Mater* **14**, 796 (2015).
- ⁹ M. Först, A. Frano, S. Kaiser, R. Mankowsky, C. R. Hunt, J. J. Turner, G. L. Dakovski, M. P. Minitti, J. Robinson, T. Loew, M. Le Tacon, B. Keimer, J. P. Hill, A. Cavalleri, and S. S. Dhesi, *Phys. Rev. B* **90**, 184514 (2014).
- ¹⁰ M. H. Hamidian, S. D. Edkins, C. K. Kim, J. C. S. Davis, A. P. Mackenzie, H. Eisaki, S. Uchida, M. J. Lawler, E. A. Kim, S. Sachdev, and K. Fujita, (2015), arXiv:1507.07865.
- ¹¹ This state is more accurately described as a d-form factor density wave. However, in this work we have chosen to refer to this state as a bond-density-wave state for the sake of succinctness.
- ¹² J. Demsar, K. Biljaković, and D. Mihailovic, *Phys. Rev. Lett.* **83**, 800 (1999).
- ¹³ J. P. Hinton, J. D. Koralek, G. Yu, E. M. Motoyama, Y. M. Lu, A. Vishwanath, M. Greven, and J. Orenstein, *Phys. Rev. Lett.* **110**, 217002 (2013).
- ¹⁴ J. P. Hinton, J. D. Koralek, Y. M. Lu, A. Vishwanath, J. Orenstein, D. A. Bonn, W. N. Hardy, and R. Liang, *Phys. Rev. B* **88**, 060508 (2013), 1305.1361.
- ¹⁵ D. H. Torchinsky, F. Mahmood, A. T. Bollinger, I. Božović, and N. Gedik, *Nat. Mater.* **12**, 387 (2013).
- ¹⁶ G. L. Dakovski, W.-S. Lee, D. G. Hawthorn, N. Garner, D. Bonn, W. Hardy, R. Liang, M. C. Hoffmann, and J. J. Turner, *Phys. Rev. B* **91**, 220506 (2015).
- ¹⁷ P. B. Littlewood and C. M. Varma, *Phys. Rev. Lett.* **47**, 811 (1981).
- ¹⁸ Higgs modes have a long history in condensed matter physics, being first observed in ^3He : D. T. Lawson, W. J. Gully, S. Goldstein, R. C. Richardson, and D. M. Lee, *Phys. Rev. Lett.* **30**, 541 (1973); D. N. Paulson, R. T. Johnson, and J. C. Wheatley, *ibid.* **30**, 829 (1973).
- ¹⁹ For a review of Higgs modes in condensed matter see e.g. D. Pekker and C. Varma, *Annual Review of Condensed Matter Physics* **6**, 269 (2015); G. E. Volovik and M. a. Zubkov, *J. Low Temp. Phys.* **175**, 486 (2014).
- ²⁰ M. A. Metlitski and S. Sachdev, *Phys. Rev. B* **82**, 075128 (2010).
- ²¹ S. Sachdev and R. La Placa, *Phys. Rev. Lett.* **111**, 027202 (2013).
- ²² K. B. Efetov, H. Meier, and C. Pépin, *Nat. Phys.* **9**, 442 (2013).
- ²³ J. D. Sau and S. Sachdev, *Phys. Rev. B* **89**, 075129 (2014).
- ²⁴ A. Allais, J. Bauer, and S. Sachdev, *Phys. Rev. B* **90**, 155114 (2014).
- ²⁵ A. Allais, J. Bauer, and S. Sachdev, *Indian J. Phys.* **88**, 905 (2014).
- ²⁶ A. Thomson and S. Sachdev, *Phys. Rev. B* **91**, 115142 (2015).
- ²⁷ Z. M. Raines, V. Stanev, and V. M. Galitski, *Phys. Rev. B* **91**, 184506 (2015).
- ²⁸ A. Moor, P. A. Volkov, A. F. Volkov, and K. B. Efetov, *Phys. Rev. B* **90**, 024511 (2014).
- ²⁹ We note that previous works (such Refs. 20 and 22) have investigated an emergent SU(2) symmetry of the superconducting and charge order, associated with particle-hole transformation on one of the hot spots. However, this emergent symmetry is explicitly broken by the curvature in the electron dispersion as well as the V term in the interaction Hamiltonian, so we do not consider its effects here.
- ³⁰ D. Chowdhury and S. Sachdev, *Phys. Rev. B* **90**, 134516 (2014).
- ³¹ P. B. Littlewood and C. M. Varma, *Phys. Rev. B* **26**, 4883 (1982).
- ³² D. A. Browne and K. Levin, *Phys. Rev. B* **28**, 4029 (1983).
- ³³ X. L. Lei, C. S. Ting, and J. L. Birman, *Phys. Rev. B* **30**, 6387 (1984).
- ³⁴ X. L. Lei, C. S. Ting, and J. L. Birman, *Phys. Rev. B* **32**, 1464 (1985).
- ³⁵ I. Tüttö and A. Zawadowski, *Phys. Rev. B* **45**, 4842 (1992).
- ³⁶ T. Cea and L. Benfatto, *Phys. Rev. B* **90**, 224515 (2014).
- ³⁷ The oscillations of the phase of superconductor are usually pushed up to plasma frequencies by coupling with the Coulomb interaction. In contrast, the phase mode of an incommensurate charge order is theoretically a Goldstone mode of the system, but in real materials this degree of freedom is usually pinned by disorder.

- ³⁸ $\Delta(\tau)$ and $\phi(\tau)$ may be treated, then, as real fields since they may always be brought to lie along the real axis via a gauge transformation.
- ³⁹ This is a parametrization in terms of longitudinal and transverse modes such as considered in Refs. 31 and 32 as opposed to radial and angular modes (c.f. Ref. 19).
- ⁴⁰ We have verified that Q^R satisfies the the Kramers-Kronig relations, both exactly in its analytic form (in terms of integrals), and approximately in our numerics for the regions of interest to within the same degree of accuracy as that of Q^R itself.
- ⁴¹ A similar framework was recently used in Ref. 36. However, the focus of that work was on the effects of the superconducting gap on the charge order, and the off-diagonal terms of \hat{Q}^R (and thus the mixing) were assumed to be small.
- ⁴² I. Kulik, O. Entin-Wohlman, and R. Orbach, *Journal of Low Temperature Physics* **43**, 591 (1981).
- ⁴³ M. Vojta and S. Sachdev, in *Advances in Solid State Physics*, *Advances in Solid State Physics Volume 41*, Vol. 41, edited by B. Kramer (Springer Berlin Heidelberg, 2001) pp. 329–341.
- ⁴⁴ In general, there is no simple time-dependent extension of Ginzburg-Landau theory, precisely due to the presence of damping, which introduces non-analytic terms (see, for example, I. J. R. Aitchison, G. Metikas, and D. J. Lee, *Phys. Rev. B* **62**, 6638 (2000), and references therein). We circumvent this difficulty by considering only the $q = 0$ limit.
- ⁴⁵ We can also add coupling to the lattice degrees of freedom, by including bi-linear terms like $g_{ep}\phi b$ and $g_{\Delta}\Delta b$, where b is a phonon mode, and g_{ep} and g_{Δ} are coupling constants.⁵² However, the effects of these couplings appear modest (see the appendix), so we will not include them.
- ⁴⁶ E. Abrahams and T. Tsuneto, *Phys. Rev.* **152**, 416 (1966).
- ⁴⁷ A. Larkin and A. Varlamov, *Theory of fluctuations in superconductors* (Clarendon Press, 2005).
- ⁴⁸ S. G. Sharapov, H. Beck, and V. M. Loktev, *Phys. Rev. B* **64**, 134519 (2001).
- ⁴⁹ W. Fu, L.-Y. Hung, and S. Sachdev, *Phys. Rev. B* **90**, 024506 (2014).
- ⁵⁰ This is consistent with the behavior of the high-energy mode in the case of strong damping from the nodal regions (see section III). This damping could lead to a decrease of the frequency of the fast mode, observed in Ref. 14 (note that a different phenomenological explanation for this decrease, based on time-independent Ginzburg-Landau theory, was given in Ref. 14).
- ⁵¹ R. Matsunaga, Y. I. Hamada, K. Makise, Y. Uzawa, H. Terai, Z. Wang, and R. Shimano, *Phys. Rev. Lett.* **111**, 057002 (2013).
- ⁵² H. Schaefer, V. V. Kabanov, and J. Demsar, *Phys. Rev. B* **89**, 045106 (2014).